Carbaborane Derivatives of the Late- and Post-transition Elements. Part 3.* Structural Consequences of Ligand Substitution in Palladadicarbadodecaboranes $3\text{-}L_2\text{-}3,1,2\text{-}PdC_2B_9H_{11}$. The Crystal and Molecular Structures of $3\text{-}[Me_2N(CH_2)_2NMe_2]\text{-}3,1,2\text{-}PdC_2B_9H_{11}$ and $3\text{-}(PMe_3)_2\text{-}3,1,2\text{-}PdC_2B_9H_{11}$†

Howard M. Colquhoun, Trevor J. Greenhough, and Malcolm G. H. Wallbridge
Department of Chemistry and Molecular Sciences, University of Warwick, Coventry, CV4 7AL

The action of $Tl^+[3,1,2\text{-}TlC_2B_9H_{11}]^-$ on $[PdCl_2(tmen)]$ [tmen = $Me_2N(CH_2)_2NMe_2$] yields the aminometallacarbaborane 3-(tmen)-3,1,2-$PdC_2B_9H_{11}$ (**1**) which possesses a 'slipped' structure, as shown by a single-crystal *X*-ray study [Pd–B 2.182(6), 2.202(5), and 2.182(6) Å and Pd–C 2.608(4) and 2.623(4) Å; *a* = 8.474 5(12), *b* = 12.363 6(19), *c* = 16.775 9(26) Å, β = 109.14(1)°, *R* = 0.03 for 2 070 independent observed reflections]. The diamine ligand may be displaced from complex (**1**) by cyclo-octa-1,5-diene, in the presence of HCl, and by trimethylphosphine, which in turn is displaced by trimethyl phosphite yielding the complexes $3\text{-}L_2\text{-}3,1,2\text{-}PdC_2B_9H_{11}$ {L_2 = 1,5-C_8H_{12}, $(PMe_3)_2$ (**2**), or $[P(OMe)_3]_2$}. The ^{11}B n.m.r. spectra are consistent with a more symmetrical structure for complex (**2**) than for (**1**) and this has been confirmed by an *X*-ray study which shows Pd–B 2.260(5), 2.315(5), and 2.249(4) Å, and Pd–C 2.414(4) and 2.492(4) Å; *a* = 6.718 3(10), *b* = 15.502 4(18), *c* = 17.918 4(24), β = 101.90(1)°, *R* = 0.026 for 2 214 independent observed reflections.

It has been shown that, in metallacarbaboranes containing the cage fragment $3,1,2\text{-}MC_2B_9H_{11}$, a progressive decrease in the extent of metal–cage bonding occurs as the number of electrons associated with the metal M increases.[1] Thus when a d^8 metal ion (*e.g.* Ni^{II},[2] Pt^{II},[3] or Au^{III}[4]) is bonded to the open C_2B_3 face of the $C_2B_9H_{11}$ cage, a distortion of the face results in a lengthening of the M–C bonds, and the so-called 'slipped' configuration arises;[5] similar distortions occur, at least in part, for the d^9 ions, Cu^{II}[6] and Au^{II}.[7] With d^{10} ions (*e.g.* Hg^{II}) the metal is co-ordinated almost linearly by a ligand (*e.g.* triphenylphosphine) and the unique boron of the C_2B_3 face, implying a mercury–boron pseudo σ bond,[8] while for the $d^{10}s^2$ thallium(I) ion no strong metal–cage bond exists, and the system may be represented formally as an ion pair $[Tl^+C_2B_9H_{11}{}^{2-}]^-$.[9] This progressive cage opening has been ascribed to increasing occupation of the $e_1{}^*$ metal–cage π-antibonding molecular orbitals ($e_1{}^* \sim d_{xz}, d_{yz}$), and it has been suggested that the introduction of π-acid ligands onto the metal could produce a more nearly closed polyhedron by delocalising electron density from $e_1{}^*$ onto the ligands.[10]

To test this proposal we have prepared a series of complexes of the form $3\text{-}L_2\text{-}3,1,2\text{-}PdC_2B_9H_{11}$ and have determined the molecular structures of two of them, 3-(tmen)-3,1,2-$PdC_2B_9H_{11}$ (**1**) and $3\text{-}(PMe_3)_2\text{-}3,1,2\text{-}PdC_2B_9H_{11}$ (**2**). These complexes differ only in the nature of the ligands L_2 in that tmen = 1,2-$(NMe_2)_2C_2H_4$ is essentially a pure σ donor, whereas PMe_3 is generally considered a moderate π acceptor.[11] A preliminary report of some of this work has been published.[12]

Results and Discussion

The reaction between $[PdCl_2(tmen)]$ and $Tl^+[3,1,2\text{-}TlC_2B_9\text{-}H_{11}]^-$ [13] in dichloromethane gave a dark green crystalline material formulated as 3-(tmen)-3,1,2-$PdC_2B_9H_{11}$ on the basis of elemental analysis, i.r., ^1H and ^{11}B n.m.r. spectroscopy. This complex proved a surprisingly versatile reagent for the preparation of other ligand derivatives $3\text{-}L_2\text{-}3,1,2\text{-}PdC_2B_9H_{11}$, since the diamine is readily displaced by alkyl- and aryl-phosphines, alkyl phosphites, isocyanides, and thioureas. A number of substitution products have been characterised as crystalline solids, including the deep red $3\text{-}(PMe_3)_2\text{-}3,1,2\text{-}PdC_2B_9H_{11}$ (**2**) and the bright orange $3\text{-}[P(OMe)_3]_2\text{-}3,1,2\text{-}PdC_2B_9H_{11}$ (**3**). In the presence of anhydrous HCl, the chelating alkene cyclo-octa-1,5-diene binds to palladium (tmen being displaced as the hydrochloride) to give the dark purple derivative $3\text{-}(1,5\text{-}C_8H_{12})\text{-}3,1,2\text{-}PdC_2B_9H_{11}$ (**4**), although under neutral conditions no reaction occurs. Indeed, the reaction of complex (**4**) with free tmen (and with other amines including $MeNH_2$ and NH_3) proceeds rapidly in the opposite direction. A series of such displacement reactions on $3\text{-}L_2\text{-}3,1,2\text{-}PdC_2B_9H_{11}$ has established the order of ligand-displacement strength as 1,5-C_8H_{12} < tmen < Bu^tNC < PMe_3 < $P(OMe)_3$. The reactions were monitored in each case by changes in the ^{11}B n.m.r. spectrum, every compound showing a low-field doublet some 6—20 p.p.m. downfield from $\delta(BF_3\cdot Et_2O)$ = 0, and a series of overlapping high-field doublets (*ca.* 7—20 p.p.m.). The actual shifts vary from one compound to another and thus provide a distinctive test of displacement. We have also prepared $3\text{-}(PMe_3)_2\text{-}3,1,2\text{-}PtC_2B_9H_{11}$ (**5**) for comparative purposes.

The ^{11}B n.m.r. spectra also allow a prediction to be made concerning the structures of the various complexes in that, for example, a dramatic difference exists between (**1**) and (**2**), with the low-field doublet (arising from one boron atom of the C_2B_9 cage, from integration measurements) of the amino-compound (**1**) being displaced some 13.3 p.p.m. upfield (from *ca.* +20.0 to +6.7 p.p.m.) for the phosphine compound (**2**). Since this resonance is particularly distinctive of the 'slipped' structure,[7] such shifts *may* be associated with the degree of distortion; the lower the shift of this doublet the greater is the distortion, as borne out by the two structures reported below. Care must obviously be exercised in making such correlations; for

* Part 2 is ref. 8.
† 3-(*NNN'N'*-Tetramethylethylenediamine)- and 3,3-bis(trimethylphosphine)-1,2-dicarba-3-palladadodecaborane, respectively.

Supplementary data available (No. SUP 56135, 19 pp.): derivation of parameter *d*, packing diagram, H-atom co-ordinates, thermal parameters, full list of bond lengths for compounds (**1**) and (**2**). See Instructions for Authors, *J. Chem. Soc., Dalton Trans.*, 1985, Issue 1, pp. xvii—xix. Structure factors are available from the editorial office.

Table 1. The ^{11}B n.m.r. shifts of a series of metallacarbaboranes

Compound	^{11}B N.m.r. shift[a]
3-(tmen)-3,1,2-$PdC_2B_9H_{11}$[b]	+20.04(1), −7.36(2), −9.30(3), −22.66(3)
3-$(PMe_3)_2$-3,1,2-$PdC_2B_9H_{11}$	+6.68(1), −8.96(3), −15.05(4), −20.30(1)
3-$[P(OMe)_3]_2$-3,1,2-$PdC_2B_9H_{11}$	+6.85(1), −7.27(3), −12.26(2), −15.65(2), −20.55(1)
3-(1,5-C_8H_{12})-3,1,2-$PdC_2B_9H_{11}$	+17.67(1), −6.93(5), −12.18(2), −23.42(1)
3-(dppe)-3,1,2-$PdC_2B_9H_{11}$	+12.77(1), −8.54(5), −17.08(3)
3-(dppe)-3,1,2-$PtC_2B_9H_{11}$	+10.32(1), −9.22(5), −22.41(3)
3-(dppe)-3,1,2-$NiC_2B_9H_{11}$	+4.99(1), −7.36(3), −14.55(4), −19.53(1)
3-$(Bu^tNC)_2$-3,1,2-$PdC_2B_9H_{11}$	+16.07(1), −3.44(1), −7.36(4), −18.18(2), −22.07(1)
3-$(NH_3)_2$-3,1,2-$PdC_2B_9H_{11}$	+13.28(1), −11.92(5), −23.68(3)
3-(Ph_4C_4)-3,1,2-$PdC_2B_9H_{11}$	+8.54(1), −6.77(5), −16.41(3)

[a] Relative to $BF_3{\cdot}Et_2O$, see Experimental section; values in brackets represent relative intensities. All signals are doublets; CH_2Cl_2 solvent. [b] CD_2Cl_2 solvent.

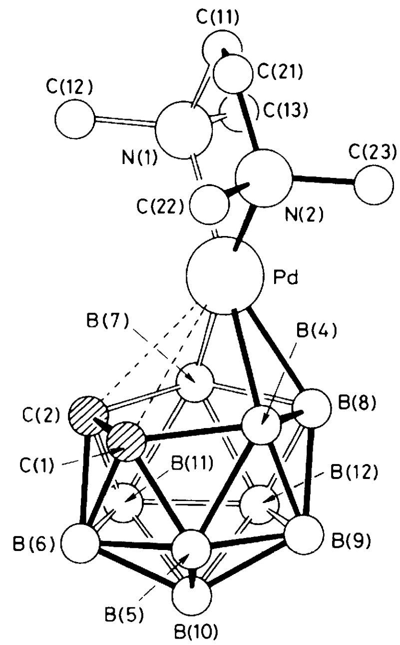

Figure 1. Molecular structure of 3-(tmen)-3,1,2-$PdC_2B_9H_{11}$ (**1**), H atoms being omitted

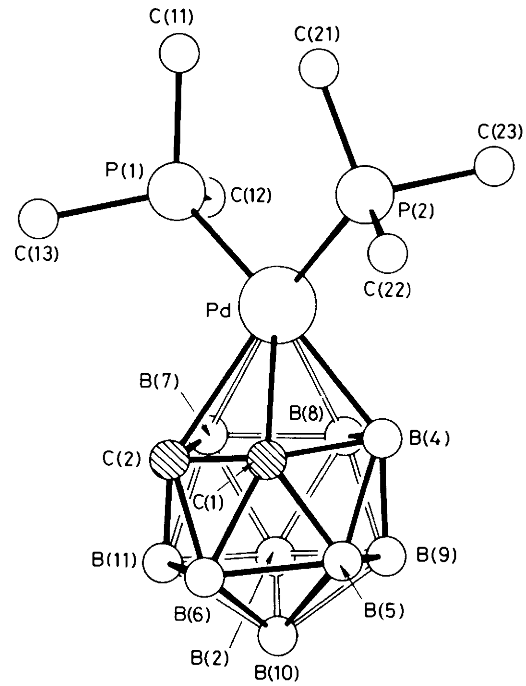

Figure 2. Molecular structure of 3-$(PMe_3)_2$-3,1,2-$PdC_2B_9H_{11}$ (**2**), H atoms being omitted

example, we have found previously that in those compounds where the metal atom is either not strongly bonded into the open C_2B_3 face, or is effectively bonded to only one of the boron atoms, as in $[TlC_2B_9H_{11}]^-$ and 3-PPh_3-3,1,2-$HgC_2B_9H_{11}$ respectively, then no low-field doublet is observed.[8] Further, while the unique boron atom within the C_2B_9 cage which is responsible for the doublet has not yet been identified conclusively, the ^{11}B–^{195}Pt coupling observed for complex (**5**) suggests that the doublet arises from the directly bonded atom B(3). The ^{11}B n.m.r. data, showing the relative shifts of the doublets obtained for the present series of compounds, are given in Table 1.

The main purpose of this investigation was to clarify whether any structural changes occur in the MC_2B_9 fragment of the 3-L_2-3,1,2-$MC_2B_9H_{11}$ compounds as the ligands L are varied. The molecular structures of (**1**) and (**2**) were therefore determined by *X*-ray diffraction, and are shown in Figures 1 and 2. The corresponding bond lengths and inter-bond angles are given in Tables 2 and 3 respectively.

Description of Structures.—The structures of both compounds show distortions of the MC_2B_9 cage from idealised icosahedral geometry, and are broadly similar to those of other compounds containing d^8 metal ions [*e.g.* Pt^{II} [3] and Au^{III} [4]]. The distortions from a 'symmetrical' structure, typified[14,15] by the rhenium(I) (d^6) complex $[3\text{-}(CO)_3\text{-}3,1,2\text{-}ReC_2B_9H_{11}]^-$, may be summarised as involving (*i*) a bending of both the upper C_2B_3 face *and* the lower B_5 pentagonal girdle of the $C_2B_9H_{11}$ fragment, (*ii*) changes in bond distances and angles, including a shortening of the C–C and a lengthening of the B–C bond distances, and a decrease in the B(7)–B(8)–B(4) angle in the C_2B_3 face, (*iii*) a shortening of the C–B(5), –B(11) bonds, and (*iv*) an asymmetry in the bonding of the palladium atom to the C_2B_3 face, in that the metal atom is more closely associated with the three boron atoms than with the carbon atoms. This last point illustrates particularly the major difference between the two structures, namely that the palladium atom is much less symmetrically positioned with respect to the C_2B_9 cage in complex (**1**) than it is in complex (**2**). The metal–cage distances for (**1**) are Pd–B(8) 2.205(5), Pd–B(4), –B(7) 2.182(6), and Pd–C 2.623(4), 2.608(4), Å, while in (**2**) the values are Pd–B(8) 2.315(5), Pd–B(4), –B(7) 2.249(4), 2.260(5), and Pd–C 2.414(4), 2.492(4) Å.

Table 2. Bond lengths (Å) with estimated standard deviations (e.s.d.s) for $(tmen)PdC_2B_9H_{11}$ (**1**) and $(PMe_3)_2PdC_2B_9H_{11}$ (**2**). Bonds to hydrogen are omitted

(*a*) Within the polyhedron

	(1)	(2)		(1)	(2)
Pd–B(4)	2.182(6)	2.249(4)	C(1)–C(2)	1.494(8)	1.513(5)
Pd–B(7)	2.182(6)	2.260(5)	C(1)–B(4)	1.769(7)	1.764(6)
Pd–B(8)	2.202(5)	2.315(5)	C(2)–B(7)	1.778(7)	1.744(6)
Pd–C(1)	2.623(4)	2.414(4)	B(7)–B(8)	1.776(8)	1.792(6)
Pd–C(2)	2.608(4)	2.492(4)	B(4)–B(8)	1.784(8)	1.758(7)
C(1)–B(6)	1.704(7)	1.745(7)	B(9)–B(12)	1.746(9)	1.747(7)
C(1)–B(5)	1.643(7)	1.662(5)	B(12)–B(11)	1.780(7)	1.774(7)
C(2)–B(6)	1.720(7)	1.704(6)	B(11)–B(6)	1.773(9)	1.760(7)
C(2)–B(11)	1.650(7)	1.658(6)	B(6)–B(5)	1.745(9)	1.781(7)
B(7)–B(11)	1.835(7)	1.816(6)	B(5)–B(9)	1.787(7)	1.774(7)
B(7)–B(12)	1.827(8)	1.804(6)	B(10)–B(12)	1.756(8)	1.782(7)
B(4)–B(9)	1.831(8)	1.807(7)	B(10)–B(11)	1.773(9)	1.772(6)
B(4)–B(5)	1.848(7)	1.804(7)	B(10)–B(6)	1.722(8)	1.757(7)
B(8)–B(12)	1.751(8)	1.769(7)	B(10)–B(5)	1.760(9)	1.785(7)
B(8)–B(9)	1.758(7)	1.775(7)	B(10)–B(9)	1.766(8)	1.755(7)

(*b*) Exo-polyhedral

	(1)		(1)		(2)		(2)
Pd–N(1)	2.170(4)	N(2)–C(21)	1.472(11)	Pd–P(1)	2.280(1)	P(1)–C(13)	1.810(5)
Pd–N(2)	2.168(4)	N(2)–C(22)	1.462(8)	Pd–P(2)	2.302(1)	P(2)–C(21)	1.811(5)
N(1)–C(11)	1.469(10)	N(2)–C(23)	1.459(7)	P(1)–C(11)	1.816(5)	P(2)–C(22)	1.818(5)
N(1)–C(12)	1.449(8)	C(11)–C(21)	1.300(14)	P(1)–C(12)	1.812(5)	P(2)–C(23)	1.806(5)
N(1)–C(13)	1.469(7)						

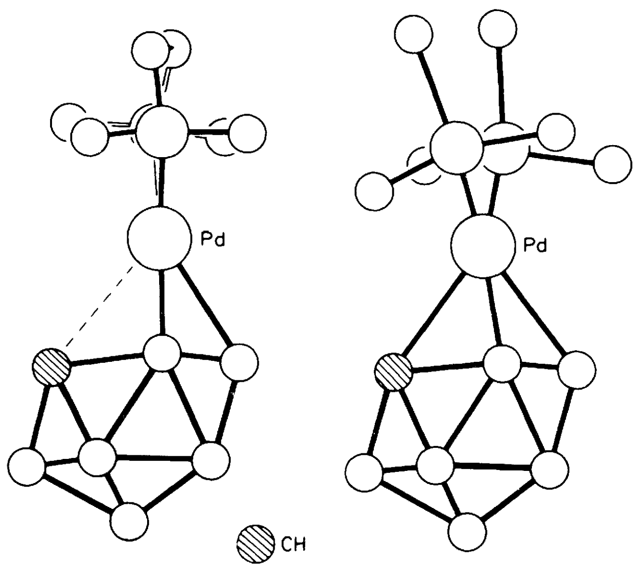

(1) (2)

Figure 3. Molecular projections of complexes (**1**) and (**2**) approximately parallel to the cage C–C bond. The C atoms in (**2**) do not quite superimpose as shown, the average being taken

The difference in the metal–cage interactions is illustrated in Figure 3.

The orientation of the PdL_2 fragment with respect to the C_2B_9 cage is similar in both compounds, and lies close to the Pd-B(4)–B(7) plane, thus resembling both 3-(Et_2NCS_2)-3,1,2-$AuC_2B_9H_{11}$[4] and 3-$(PEt_3)_2$-3,1,2-$PtC_2B_9H_{11}$.[3] However, the Pd-P_2 plane in complex (**2**) is rotated by *ca.* 13° with respect to the Pd-B(4)–B(7) plane, while the Pd-N_2 plane in (**1**) shows a rotation of only *ca.* 2°, in the opposite sense. This is illustrated in Figure 4, and the greater rotation in (**2**) almost certainly arises

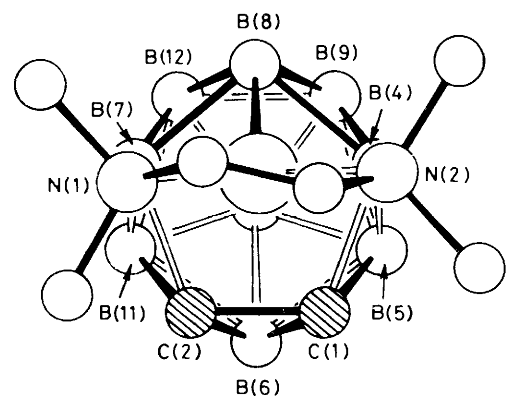

(*a*)

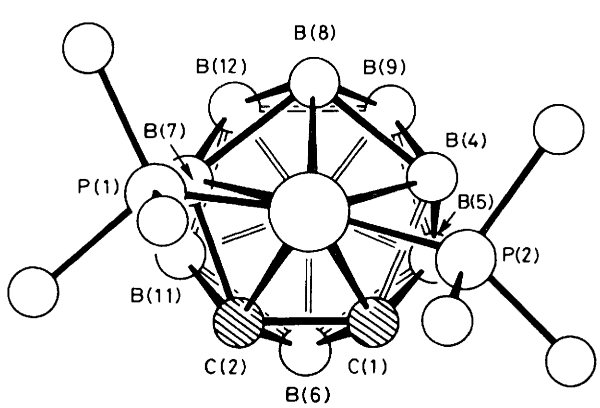

(*b*)

Figure 4. Molecular projections perpendicular to the B(5)–B(9)–B(12)–B(11) plane for (*a*) (**1**) and (*b*) (**2**)

Table 3. Inter-bond angles (°) and e.s.d.s

(*a*) Within the polyhedron

	(1)	(2)		(1)	(2)
C(2)–Pd–C(1)	33.2(1)	35.9(1)	C(1)–C(2)–B(6)	63.6(3)	65.4(3)
C(2)–Pd–B(7)	42.4(2)	42.7(2)	B(6)–C(1)–C(2)	64.7(4)	62.6(3)
C(1)–Pd–B(4)	42.0(2)	44.3(1)	B(4)–C(1)–B(5)	65.5(3)	63.5(3)
B(4)–Pd–B(8)	48.0(2)	45.3(2)	B(7)–C(2)–B(11)	64.6(3)	64.5(3)
B(7)–Pd–B(8)	47.8(2)	46.1(2)	B(5)–C(1)–B(6)	62.8(3)	63.0(3)
Pd–C(1)–B(4)	55.5(3)	62.9(2)	B(11)–C(2)–B(6)	63.5(3)	63.1(3)
Pd–C(2)–B(7)	55.9(3)	61.5(2)	B(5)–B(4)–C(1)	54.0(3)	55.5(2)
Pd–C(1)–C(2)	72.9(3)	74.9(2)	B(11)–B(7)–C(2)	54.3(3)	55.5(2)
Pd–C(2)–C(1)	73.9(3)	69.2(2)	B(9)–B(4)–B(5)	58.1(3)	58.8(3)
Pd–B(4)–C(1)	82.5(3)	72.8(2)	B(12)–B(7)–B(11)	58.2(3)	58.7(2)
Pd–B(7)–C(2)	81.7(3)	75.7(2)	B(8)–B(4)–B(9)	58.2(3)	59.7(3)
Pd–B(7)–B(8)	66.7(3)	68.6(2)	B(8)–B(7)–B(12)	58.1(3)	58.9(2)
Pd–B(4)–B(8)	66.6(3)	69.3(2)	B(7)–B(8)–B(12)	62.4(3)	60.9(2)
Pd–B(8)–B(4)	65.4(2)	65.4(2)	B(4)–B(8)–B(9)	62.3(3)	61.5(3)
Pd–B(8)–B(7)	65.6(2)	65.4(2)	B(12)–B(8)–B(9)	59.7(3)	59.1(3)
C(1)–B(5)–B(4)	60.6(3)	61.0(3)	B(6)–B(10)–B(11)	61.0(4)	59.8(3)
B(4)–B(5)–B(9)	60.5(3)	60.7(3)	B(11)–B(10)–B(12)	60.6(3)	59.9(3)
B(9)–B(5)–B(10)	59.7(3)	59.1(3)	B(12)–B(10)–B(9)	59.4(3)	59.2(3)
B(10)–B(5)–B(6)	58.8(3)	59.1(3)	B(9)–B(10)–B(5)	60.9(3)	60.1(3)
B(6)–B(5)–C(1)	60.3(3)	60.8(3)	B(5)–B(10)–B(6)	60.1(4)	60.4(3)
C(2)–B(6)–C(1)	51.7(3)	52.0(2)	C(2)–B(11)–B(7)	61.1(3)	60.0(3)
C(1)–B(6)–B(5)	56.9(3)	56.2(2)	B(7)–B(11)–B(12)	60.7(3)	60.3(3)
B(5)–B(6)–B(10)	61.0(4)	60.6(3)	B(12)–B(11)–B(10)	59.2(3)	60.3(3)
B(10)–B(6)–B(11)	60.9(4)	60.5(3)	B(10)–B(11)–B(6)	58.1(3)	59.7(3)
B(11)–B(6)–C(2)	56.4(3)	57.2(3)	B(6)–B(11)–C(2)	60.2(3)	59.7(3)
B(8)–B(9)–B(4)	59.6(3)	58.8(3)	B(7)–B(12)–B(8)	59.5(3)	60.2(2)
B(4)–B(9)–B(5)	61.4(3)	60.5(3)	B(8)–B(12)–B(9)	60.4(3)	60.7(3)
B(5)–B(9)–B(10)	59.4(3)	60.8(3)	B(9)–B(12)–B(10)	60.6(3)	59.6(3)
B(10)–B(9)–B(12)	60.0(3)	61.2(3)	B(10)–B(12)–B(11)	60.2(3)	59.8(3)
B(12)–B(9)–B(8)	60.0(3)	60.3(3)	B(11)–B(12)–B(7)	61.2(3)	61.0(2)
C(2)–C(1)–B(4)	109.7(4)	113.1(3)	B(12)–B(9)–B(5)	106.8(4)	107.9(3)
C(1)–C(2)–B(7)	110.4(4)	108.6(3)	B(9)–B(12)–B(11)	108.0(4)	107.2(4)
C(2)–B(7)–B(8)	109.0(4)	108.5(3)	B(12)–B(11)–B(6)	108.4(4)	109.9(3)
C(1)–B(4)–B(8)	109.4(4)	106.4(3)	B(9)–B(5)–B(6)	109.6(5)	108.8(3)
B(4)–B(8)–B(7)	99.2(4)	102.3(3)	B(5)–B(6)–B(11)	106.2(4)	105.5(3)

(*b*) Exo-polyhedral

	(1)		(1)		(2)		(2)
N(1)–Pd–N(2)	83.7(2)	C(11)–N(1)–C(13)	107.2(5)	P(1)–Pd–P(2)	101.5(4)	C(11)–P(1)–C(12)	101.9(2)
Pd–N(1)–C(11)	103.8(4)	C(12)–N(1)–C(13)	107.5(5)	Pd–P(1)–C(11)	122.5(1)	C(11)–P(1)–C(13)	101.9(2)
Pd–N(1)–C(12)	113.1(3)	C(21)–N(2)–C(22)	109.3(5)	Pd–P(1)–C(12)	111.2(1)	C(12)–P(1)–C(13)	103.9(2)
Pd–N(1)–C(13)	112.8(3)	C(21)–N(2)–C(23)	112.4(5)	Pd–P(1)–C(13)	113.3(2)	C(21)–P(2)–C(22)	99.8(2)
Pd–N(2)–C(21)	104.0(5)	C(22)–N(2)–C(23)	107.0(5)	Pd–P(2)–C(21)	124.9(2)	C(21)–P(2)–C(23)	102.1(2)
Pd–N(2)–C(22)	113.4(3)	C(11)–C(21)–N(2)	120.7(8)	Pd–P(2)–C(22)	112.6(2)	C(22)–P(2)–C(23)	103.4(3)
Pd–N(2)–C(23)	110.8(4)	C(21)–C(11)–N(1)	120.3(7)	Pd–P(2)–C(23)	111.6(2)		
C(11)–N(1)–C(12)	112.4(5)						

from a packing effect. The consequences of this rotation in terms of the concomitant asymmetry in the Pd–C bond distances in (**2**), and the metal–cage bonding, are discussed below. The asymmetry in the Pd–C distances in complex (**2**) is coupled with a displacement of C(2) out of the C(1)–B(4)–B(7) plane, with C(2)–B(6) being shorter than C(1)–B(6).

The C_2B_9 framework distances in complexes (**1**) and (**2**) are generally similar to those in other distorted d^8, 3,1,2-$MC_2B_9H_{11}$, metallacarbaboranes, with the characteristic C–C distance *ca.* 1.5 Å, as compared to *ca.* 1.6 Å in symmetrically bonded structures such as [3-$(CO)_3$-3,1,2-$ReC_2B_9H_{11}$]$^-$.[14,15] Apart from the placement of the metal atom in (**1**) and (**2**), and the C(1)–B(6) distance referred to above, the major difference between the two structures is in the dihedral angle of the C_2B_3 face, which is 14.5° for (**1**) and 9.7° for (**2**) (planes 1 and 2, Table 4). The B_5-girdle dihedral angles (planes 3 and 4, Table 4) are 9.6 and 8.1° for (**1**) and (**2**) respectively, similar to those in other d^8 3,1,2-$MC_2B_9H_{11}$ compounds such as 3-(Et_2NCS_2)-3,1,2-$AuC_2B_9H_{11}$ (9.2°),[4] [Au$(C_2B_9H_{11})_2$]$^-$ (8.4°),[16] and 3-$(PEt_3)_2$-3,1,2-$PtC_2B_9H_{11}$ (7.9°).[3] A summary of the distortions which occur in a variety of MC_2B_9 metallacarbaboranes is given in Table 5 and discussed in more detail below.

The amine ligand in complex (**1**) exhibits some unlikely bond distances and inter-bond angles,[17] and it would appear that two alternative configurations are present, this disorder being characterised by the abnormally large thermal parameters and the short C(11)–C(21) distance of 1.30(1) Å. An unsuccessful attempt was made to introduce the two possible configurations

Table 4. Some best least-squares planes

	Plane 1	(1)	(2)	Plane 2	(1)	(2)	Plane 3	(1)	(2)
Atoms defining the plane (unit weight) and deviation (Å) from the plane	C(1)	−0.005	0.040	B(4)	0	0	B(11)	0.002	0.011
	C(2)	0.005	−0.039	B(7)	0	0	B(12)	−0.003	−0.017
	B(4)	0.003	−0.060	B(8)	0	0	B(9)	0.003	0.017
	B(7)	−0.003	0.059				B(5)	−0.002	−0.011
σ		0.005	0.058		0	0		0.003	0.017
Other atoms and deviations (Å)	Pd	1.701	−1.826	Pd	1.690	−1.731	Pd	3.294	−3.304
	H(1)	0.579	−0.433	H(4)	0.369	−0.375	H(11)	−0.328	0.449
	H(2)	0.558	−0.458	H(7)	0.346	−0.344	H(12)	−0.553	0.472
	H(4)	0.335	−0.398	H(8)	0.441	−0.478	H(8)	−0.545	0.523
	H(7)	0.333	−0.405				H(5)	−0.296	0.379

	Plane 4	(1)	(2)	Plane 5	(1)	Plane 6	(2)	Plane 7	(2)
Atoms defining the plane (unit weight) and deviation (Å) from the plane	B(6)	0	0	Pd	0.009	Pd	0	Pd	0
	B(11)	0	0	N(1)	0.023	P(1)	0	B(4)	0
	B(5)	0	0	N(2)	−0.028	P(2)	0	B(7)	0
				B(4)	0.025				
				B(7)	−0.029				
σ		0	0		0.027		0		0
Other atoms and deviations (Å)	Pd	3.108	−3.188			B(4)	−0.438	P(1)	−0.527
	H(6)	−0.250	0.280			B(7)	0.084	P(2)	0.191
	H(11)	−0.273	0.375						
	H(5)	−0.236	0.332						

Acute angles (°) between the planes

	Planes	Angle	Planes	Angle		Planes	Angle	Planes	Angle	Planes	Angle
(1)	1–2	14.5	2–3	5.6	(2)	4–7	87.0	1–7	85.9	2–4	10.8
	1–3	8.9	2–4	15.2		1–2	9.7	4–6	86.2	2–6	83.1
	1–4	0.7	2–5	81.7		1–3	6.9	3–7	79.0	2–7	76.3
	1–5	83.7	3–4	9.6		1–4	1.2	6–7	13.5	3–4	8.1
	4–5	83.1	3–5	87.3		1–6	87.4	2–3	2.8	3–6	85.8

into the model. The Pd–N distance in (**1**) of 2.17 Å is 0.17 Å longer than that expected for Pd^{II} bonded to an sp^3-hybridised nitrogen atom,[18] indicating a considerable *trans* effect from the $C_2B_9H_{11}$ cage. The Pd–P distance in (**2**) (average 2.29 Å), on the other hand, is shorter than predicted from the sum of covalent radii,[19] but is comparable with the value observed in other phosphine–palladium compounds.[20,21] The other values of bond distances and angles within the amine and phosphine ligands are in agreement with those found in similar compounds.

The only non-bonded intermolecular contacts which are interestingly short are H ··· H, and these are listed in Table 6. Examination of these distances clearly reveals that while the Pd–N_2 plane in (**1**) is stabilised approximately in the Pd–B(4)–B(7) plane, the contacts in (**2**) dictate the observed rotation of the Pd–P_2 plane by *ca.* 13° with respect to the Pd–B(4)–B(7) plane.

Molecular Distortions in Metallacarbaboranes of the Type 3,1,2-$MC_2B_9H_{11}$.—The projections given in Figure 4 have been chosen in the light of much recent information and discussion on the geometrical interpretation of distorted 3,1,2-$MC_2B_9H_{11}$ compounds. We have suggested that the original description of these distortions in terms of 'slipped' structures is inadequate due to the accompanying framework distortions which occur in the C_2B_9 fragment[4] and subsequently it has been suggested that a new 'slip' parameter, Δ, be used, based on the lower B_5 pentagonal girdle of the C_2B_9 cage, coupled with two angles, θ and φ, to define one of the major distortions of this cage, namely the folding of the C_2B_3 open face.[3] This is one of many possible geometrical descriptions relating the observed structures to their *hypothetical* symmetrically bonded equivalents.

A survey of a range of the 3,1,2-$MC_2B_9H_{11}$ metallacarbaboranes from the symmetrically bonded d^6 [rhenium(I)] compounds through the distorted d^8—d^{10} systems to the essentially non-bonded ion pair in the $d^{10}s^2$ ion $[TlC_2B_9H_{11}]^-$ (see Table 5) indicates that a full description of these structures requires a consideration of *all* the metal–cage and framework parameters. However, while a simpler description, using only a few parameters, would obviously be useful for comparative purposes, a common reference standard applicable to all structures is required initially.

Although the lower B_5 pentagonal girdle [B(5), B(6), B(11), B(12), B(9), Figure 1] appears to provide a suitable reference frame in which a 'slip' parameter such as Δ can be measured,[3] it is evident from Table 5 that the planarity exhibited by this fragment in the ion $[3\text{-}(CO)_3\text{-}3,1,2\text{-}ReC_2B_9H_{11}]^-$ [14,15] is not generally maintained; indeed, in the d^8 compounds, it is characterised by a remarkably constant B_3/B_4 dihedral angle (planes 3 and 4, Table 4) of 8—10°.

Considering all the structurally characterised 3,1,2-$MC_2B_9H_{11}$ compounds, we have determined a distortion parameter d by taking the B_4 unit [B(11)–B(12)–B(9)–B(5)] of the lower B_5 girdle as the most suitable reference plane since this is the least distorted fragment in the C_2B_9 cage, the geometry and planarity remaining essentially constant over all the known compounds. Also, in no case does it differ significantly from the same fragment in the $[3,1,2\text{-}TlC_2B_9H_{11}]^-$ ion[9] which gives the best indication to date of the geometry of the non-co-ordinated [7,8-

Table 5. Metal–cage distances (Å) and framework distortions in 3,1,2-$MC_2B_9H_{11}$ complexes

	d^6 [a]Re^I	d^7 [b]Ni^{III}	d^8 [c]Pd^{II} (2)	d^8 [d]Pt^{II}	d^8 [c]Pd^{II} (1)	d^8 [e]Au^{III}	d^8 [f]Au^{III}	d^9 [g]Cu^{II}	d^{10} [h]Hg^{II}	$d^{10}s^2$ [i]Tl^I
M–B(8) [j]	2.35	2.16	2.32	2.26	2.20	2.20	2.20	2.13	2.20	2.66
M–B(4), B(7) [j]	2.34	2.11	2.25	2.28	2.18	2.22	2.26	2.23	2.52	2.74
M–C	2.31	2.15	2.45	2.57	2.61	2.79	2.78	2.58	2.90	2.92
C_2B_3 face dihedral angle (°) (acute, positive)	0.2	5.1	9.7	9.0	14.5	17.2	13.6	8.0	5.2	3.6
Lower B_5 girdle dihedral angle (°) (acute, positive)	0.8	5.1	8.1	7.9	9.6	9.2	8.4	4.2	0.5	0.3
d/Å	0.04	0.01	0.11	0.27	0.36	0.53	0.55	0.47	0.94	
Δ/Å	0.05	0.09	0.26	0.42	0.52	0.68	0.69	0.54	0.92	
C–C	1.61	1.59	1.51	1.53	1.49	1.46	1.50	1.53	1.54	1.56
Facial B–C [j]	1.71	1.72	1.77	1.75	1.77	1.82	1.75	1.69	1.60	1.64
B(7)–B(11), B(12) [j]; B(4)–B(5), B(9)	1.77	1.80	1.81	1.82	1.84	1.84	1.81	1.82	1.78	1.77
B(7)–B(8)–B(9) °	106	105	102	101	99	98	98	99	101	105
C–B(5), B(11) [j]	1.73	1.70	1.66	1.66	1.65	1.62	1.64	1.71	1.69	1.72

[a] $[(3\text{-}CO)_3\text{-}3,1,2\text{-}ReC_2B_9H_{11}]^-$.[15] [b] $[N(CH_3)_4]^+[Ni(1,2\text{-}C_2B_9H_{11})_2]^-$ (F. V. Hansen, R. G. Hazell, C. Hyatt, and G. D. Stucky, *Acta Chem. Scand.*, 1973, **27**, 1210). [c] This work. [d] $3,3\text{-}(PEt_3)_2\text{-}3,1,2\text{-}PtC_2B_9H_{11}$.[3] [e] $3\text{-}Et_2NCS_2\text{-}3,1,2\text{-}AuC_2B_9H_{11}$.[25] [f] $[Au(Et_2NCS_2)_2]^+[Au(1,2\text{-}C_2B_9H_{11})_2]^-$.[16] [g] $[NEt_4]_2{}^{2+}[Cu(1,2\text{-}C_2B_9H_{11})_2]^{2-}$.[6] [h] $3\text{-}PPh_3\text{-}3,1,2\text{-}HgC_2B_9H_{11}$.[1] [i] $[PPh_3Me]^+[3,1,2\text{-}TlC_2B_9H_{11}]^-$.[9] [j] Mean values.

Table 6. Intermolecular H ··· H contact distances (Å) < 2.5 Å

(1)		(2)	
H(5) ··· H(133^I)	2.38	H(9) ··· H(1^I)	2.22
H(223) ··· H(131^{II})	2.42	H(8) ··· H(213^I)	2.38
H(8) ··· H(132^{II})	2.42	H(9) ··· H(223^I)	2.28
H(8) ··· H(231^{II})	2.24	H(12) ··· H(2^I)	2.35
H(10) ··· H(222^{III})	2.37		
H(10) ··· H(1^{III})	2.32		
H(11) ··· H(221^{IV})	2.47		
H(123) ··· H(232^{V})	2.38		

Symmetry codes: I $1 + x, y, z$; II $-x, -y, -z$; III $1 - x, y - \frac{1}{2}, \frac{1}{2} - z$; IV $x, \frac{1}{2} - y, \frac{1}{2} + z$

$C_2B_9H_{11}]^{2-}$ ion. Thus, in Figure 4, the views are perpendicular to the best least-squares plane through these four atoms. This plane (common to all the known structures), together with the dihedral angles of the C_2B_3 and B_5 planes, allows the use of a minimum number of parameters to convey the general geometric features of the structures consistent with the actual distortions present.

In referring the metal atom position to the B_4 plane,* it is not intended that any conclusions be drawn concerning the hypothetical structure which has the metal symmetrically positioned with respect to the atoms of this plane; the d parameter derived (Table 5) refers only to the projection of the metal atom on to the B_4 plane. Clearly, if the metal projection is symmetrically placed with respect to the four atoms of this plane ($d = 0$), then it is also similarly placed with respect to all five atoms of the plane when distortions are removed and B(6) is returned to the B_4 plane, as in the symmetrically bonded rhenium compound, and in the essentially non-co-ordinated $[7,8\text{-}C_2B_9H_{11}]^{2-}$ ion.

The framework distortions, given in Table 5, are evidently maximised at the d^8 configuration, the d^{10} mercury(II) compound being anomalous in that the mercury atom is only bonded essentially to one boron atom in the C_2B_3 face.[8] The largest distortions, apart from the non-planarities of the C_2B_3 face and the B_5 girdle, as represented by their dihedral angles, occur in the bond lengths involving the two carbon atoms. The various C_2B_9 parameters show an interesting correlation with the dihedral angles, so that the framework distortions are well represented by these two dihedral angles or the facial/non-facial bond distances given in Table 5. Angles θ' and φ', based on the B_4 plane and analogous to θ and φ,[3] could equally well be used to represent the framework distortions; it is noteworthy that θ and φ, based on the B_5 plane, generally show $\theta < \varphi$, suggesting that the greater framework distortion is in the facial B_3 region, while the angles θ' and φ' generally give $\theta' > \varphi'$, which is more consistent with the observed framework distortions.

Since in complex (**1**), and particularly in (**2**), M–B(8) is longer than M–B(4), B(7), it is clear that framework distortions are as important, if not more so, as any single general descriptive term for the deformation, such as 'slip' which implies M–B(8) < M–B(4), B(7). Further, since the d parameter is smaller than Δ, and is especially small for (**2**) here, this appears to be a better descriptive parameter since the cage deformations then assume the importance which is evident from the metal–cage distances.

The bonding in $MC_2B_9H_{11}$ compounds has recently been discussed in detail, and allows an understanding of the observed distortions.[2] Both (**1**) and (**2**) possess 18-electron configurations, counting the $C_2B_9H_{11}{}^{2-}$ ion as a six-electron donor, and for a symmetrically placed d^8 metal ion the dominant bonding interaction involves metal hybrid (xz) and cage $5e_1$ (a'') orbitals. The filled metal (yz) orbital enters into a four-electron antibonding interaction with the cage $5e_1$ (a') orbital. It is this interaction which could be reduced by the effect of π-acceptor ligands lying in the yz plane, as is the case in complex (**2**), yielding a more nearly icosahedral geometry than is observed in (**1**), and thus confirming earlier predictions.[10] Relatively few results are available to test the prediction further, although it has recently been shown that an analogous rhodium(I) complex (also d^8) has an essentially undistorted structure.[22] This result was ascribed both to the presence of a carbonyl ligand (π acceptor) on rhodium, and to the smaller d–p promotion energy

* The actual procedure used to derive the distortion parameter d is described in SUP 56135. In practice, if the distance of the co-ordinate centroid of the B_4 unit from the projection of the metal atom onto the B_4 plane is d_2, then $d = d_2 + 0.376$ Å.

Table 7. Final atomic co-ordinates (× 10^5 for Pd, × 10^4 for others) for the non-hydrogen atoms in (tmen)$PdC_2B_9H_{11}$ (**1**) and $(PMe_3)_2PdC_2B_9H_{11}$ (**2**) with e.s.d.s in parentheses

Atom	*x*	*y*	*z*	Atom	*x*	*y*	*z*
Complex (**1**)				Complex (**2**)			
Pd	20 192(4)	15 932(3)	10 001(2)	Pd	31 296(4)	19 586(2)	30 819(2)
C(1)	5 057(5)	1 270(3)	2 038(3)	C(1)	3 701(5)	2 983(3)	4 119(2)
C(2)	3 918(6)	1 264(3)	2 555(3)	C(2)	3 084(5)	3 521(3)	3 404(2)
B(4)	4 135(6)	538(4)	1 093(3)	B(4)	5 688(7)	2 254(3)	4 073(3)
B(5)	5 929(7)	92(5)	2 000(4)	B(5)	5 990(7)	3 239(3)	4 622(3)
B(6)	5 747(8)	546(4)	2 951(4)	B(6)	4 341(7)	4 075(3)	4 181(3)
B(7)	2 080(7)	510(4)	2 036(3)	B(7)	4 507(7)	3 192(3)	2 744(2)
B(8)	2 346(6)	−170(4)	1 156(3)	B(8)	6 430(7)	2 456(3)	3 205(3)
B(9)	4 281(7)	−839(4)	1 513(3)	B(9)	7 745(6)	2 993(4)	4 036(3)
B(10)	5 135(8)	−753(4)	2 623(4)	B(10)	6 880(7)	4 058(3)	4 071(3)
B(11)	3 787(7)	74(4)	2 975(3)	B(11)	4 877(7)	4 203(3)	3 267(3)
B(12)	2 966(6)	−849(4)	2 124(3)	B(12)	7 017(7)	3 567(3)	3 184(3)
N(1)	−77(5)	2 623(3)	963(2)	P(1)	1 366(1)	1 779(1)	1 861(1)
N(2)	2 069(5)	2 562(4)	−69(2)	P(2)	2 025(2)	794(1)	3 683(1)
C(11)	−411(10)	3 228(7)	171(5)	C(11)	−346(7)	877(3)	1 576(2)
C(12)	268(7)	3 328(6)	1 691(4)	C(12)	3 071(7)	1 691(3)	1 202(3)
C(13)	−1 595(6)	2 008(5)	902(4)	C(13)	−236(7)	2 691(3)	1 506(3)
C(21)	775(11)	339(8)	−148(5)	C(21)	−349(7)	228(3)	3 347(3)
C(22)	3 675(8)	3 094(5)	59(4)	C(22)	1 771(8)	1 041(3)	4 651(3)
C(23)	1 724(8)	1 897(6)	−825(3)	C(23)	3 853(8)	−75(3)	3 811(3)

of rhodium relative to palladium, since the four-electron metal–cage antibonding interaction can also be reduced *via d–p* hybridisation, which directs 'metal' (d_{yz}) electron density away from the cage.[3] This latter effect may also be responsible for the reduced level of distortion observed (Table 5) in the palladium complex (**2**) when compared to its platinum analogue 3,3-$(PEt_3)_2$-3,1,2-$PtC_2B_9H_{11}$, the *d–p* promotion energy of palladium(II) in a neutral complex being lower than that of platinum(II) in the same environment.[23] Finally, the cyclobutadiene–palladium complex 3-Ph_4C_4-3,1,2-$PdC_2B_9H_9Me_2$ is reported[24] to be 'symmetrically bonded,' although full details of the structure have not yet been published. In this molecule the delocalisation of e_1* (d_{yz}) electron density onto the cyclobutadiene ligand must be so extensive that the complex could in fact be regarded as one containing $Ph_4C_4{}^{2-}$ and (d^6) palladium(IV).

Experimental

Instrumentation and techniques were as previously described.[25] The starting materials [$PdCl_2$(tmen)],[26] [$PdCl_2(PMe_3)_2$],[27] and Tl^+[3,1,2-$TlC_2B_9H_{11}$]$^-$ [13] were prepared by literature methods, and 3-(C_4Ph_4)-3,1,2-$PdC_2B_9H_{11}$ [24] was obtained by reaction of Tl^+[3,1,2-$TlC_2B_9H_{11}$]$^-$ with [{$PdCl_2(C_4Ph_4)$}$_2$]. Boron-11 chemical shifts were measured at 28.9 MHz relative to external BF_3·Et_2O, and downfield shifts are quoted as positive. Microanalyses were by Butterworth Microanalytical Ltd., and C.H.N. Ltd., Leicester.

Preparations.—3-(tmen)-3,1,2-$PdC_2B_9H_{11}$ (**1**). To a stirred suspension of Tl^+[3,1,2-$TlC_2B_9H_{11}$]$^-$ (0.61 g, 1.13 mmol) in dichloromethane (100 cm^3) was added [$PdCl_2$(tmen)] (0.32 g, 1.10 mmol), and the reaction mixture stirred at room temperature for 1 h. After filtration, the resulting green solution afforded 0.22 g of a dark green crystalline solid on evaporation to dryness under reduced pressure. The aminometallacarbaborane (**1**) was purified by column chromatography on silica gel, with dichloromethane as eluant, and recrystallised from dichloromethane–pentane, giving 0.10 g (28%) of dark green crystals, m.p. > 300 °C (Found: C, 27.3; H, 7.5; B, 27.8. Calc. for $C_8H_{27}B_9N_2Pd$: C, 27.1; H, 7.6; B, 27.4%). The i.r. spectrum (Nujol) contained peaks at 3 050w, 2 541s, 2 498s, 1 283w, 1 123m, 1 014m, 955m, 801s, 768m, 738w, and 687w cm^{-1} and the ^1H n.m.r. spectrum (CD_2Cl_2) showed resonances at τ 6.43 (s, br, 2 H, carbaborane CH), 7.16 (s, 4 H, methylene groups), and 7.27 (s, 12 H, methyl groups).

3-$(PMe_3)_2$-3,1,2-$PdC_2B_9H_{11}$ (**2**). *Method* (*a*). On passing gaseous trimethylphosphine into a solution of complex (**1**) (0.015 g, 0.042 mmol) in dichloromethane (10 cm^3), the initially dark green solution became brown and then deep red. When no further change was observed, dark red crystals of the product were precipitated by dropwise addition of hexane, filtered off, washed with diethyl ether–acetone, and dried *in vacuo*. The yield of complex (**2**) was 0.017 g (*ca.* 100%), m.p. 149 °C (Found: C, 26.5; H, 7.9. Calc. for $C_8H_{29}B_9P_2Pd$: C, 24.6; H, 7.4%). The ^1H n.m.r. spectrum of the sample analysed showed it to contain a small amount of ether, accounting for the high C,H analysis figures. The ^1H n.m.r. spectrum (CD_2Cl_2) showed resonances at τ 7.24 (s, br, 2 H, carbaborane CH) and 8.37 {t, 18 H, ^2J(PH) + ^4J(PH) = 9.68, [^2J(PH) + ^4J(PH)]/J(PP′) = 1.76 Hz, methyl protons}.

Method (*b*). Reaction of [$PdCl_2(PMe_3)_2$] (1.73 mmol) with Tl^+ [3,1,2-$TlC_2B_9H_{11}$]$^-$ (1.75 mmol, CH_2Cl_2, 25 °C, 1 h) gave a dark brown solution from which crystals of complex (**2**) (0.12 g, 18%) were obtained by slow addition of diethyl ether, and identified by ^{11}B n.m.r. spectroscopy.

3-[$P(OMe)_3$]$_2$-3,1,2-$PdC_2B_9H_{11}$ (**3**). Trimethyl phosphite was added dropwise with stirring to a solution of complex (**1**) (0.036 g, 0.102 mmol) in dichloromethane, until the colour of the solution had changed from dark green to bright orange. Addition of diethyl ether precipitated a brown solid which was recrystallised from dichloromethane–pentane yielding 0.015 g (30%) of complex (**3**), m.p. 123 °C (Found: C, 19.7; H, 6.0. Calc. for $C_8H_{29}B_9O_3P_2Pd$: C, 19.8; H, 6.0%). The ^1H n.m.r. spectrum ($CDCl_3$) showed resonances at τ 6.81 (s, br, 2 H, carbaborane CH) and 6.26 [t, 18 H, ^2J(PH) + ^4J(PH) = 12.62 Hz, methyl protons], and the ^{11}B n.m.r. spectrum showed B–H doublets at δ +6.85 (1 B), −7.27 (3 B), −12.26 (2 B), −15.65 (2 B), and −20.55 (1 B).

3-(1,5-C_8H_{12})-3,1,2-$PdC_2B_9H_{11}$ (**4**). Dry HCl was passed into a dichloromethane solution (50 cm^3) containing complex (**1**) (0.18 g, 0.50 mmol) and cyclo-octa-1,5-diene (1 cm^3), the solution slowly changing from green to brown, then purple-red. The solution was filtered to remove precipitated tmen·2HCl, and diethyl ether added dropwise to the filtrate, giving 0.12 g (70%) of complex (**4**) as a deep purple crystalline solid, m.p. > 300 °C (Found: C, 33.5; H, 6.5. Calc. for $C_{10}H_{23}B_9Pd$: C, 34.7; H, 6.6%). The ^{11}B n.m.r. spectrum contained doublets at δ +17.67 (1 B), −6.93 (5 B), −12.18 (2 B), and −23.42 (1 B).

$3-(PMe_3)_2-3,1,2-PtC_2B_9H_{11}$ (**5**). This compound was obtained in essentially quantitative yield, by reaction of $[PtCl_2(PMe_3)_2]$ with $Tl^+[3,1,2-TlC_2B_9H_{11}]^-$ as described for the palladium analogue (**2**), method (*b*), and was isolated as an orange crystalline solid by recrystallisation from CH_2Cl_2–Et_2O, m.p. 190 °C (Found: C, 20.2; H, 6.0. Calc. for $C_8H_{29}B_9P_2Pt$: C, 20.0; H, 6.1%). The ^{11}B n.m.r. spectrum ($CDCl_3$) contained doublets at δ +7.19 (1 B), −9.13 (3 B), −13.28 (2 B), and −20.80 (3 B), the signal at lowest field showing platinum–boron coupling, $J(^{195}Pt-^{11}B)$ = 240 ± 10 Hz.

$3-(dppe)-3,1,2-PdC_2B_9H_{11}$ *and the corresponding nickel and platinum compounds.* An excess of dppe = $Ph_2P(CH_2)_2PPh_2$ was added to a solution of complex (**1**) (0.014 g, 0.04 mmol) in CH_2Cl_2 (2 cm^3). After 10 min, dark red crystals were precipitated by the addition of hexane, and after decantation were washed with ether and dried under vacuum. Yield, 0.025 g (98%) (Found: C, 51.7; H, 5.4. Calc. for $C_{28}H_{35}B_9P_2Pd$: C, 52.7; H, 5.5%). The nickel and platinum compounds were prepared for comparative purposes from the appropriate diphosphine metal dichloride, $[MCl_2(dppe)]$ (0.10 mmol) where M = Ni or Pt, by treatment with $Tl_2C_2B_9H_{11}$ (0.11 mmol) in dichloromethane solution (10 cm^3). After filtration to remove the precipitated TlCl the $(dppe)MC_2B_9H_{11}$ compounds were precipitated from the filtrate by addition of light petroleum. The nickel compound was obtained as dark brown crystals in yields of 50—60% (Found: C, 56.8; H, 5.8; B, 16.4. Calc. for $C_{28}H_{35}B_9NiP_2$: C, 56.9; H, 5.9; B, 16.4%). The platinum compound is a yellow crystalline solid, obtained in 40—50% yield (Found: C, 46.3; H, 5.1; B, 13.0. Calc. for $C_{28}H_{35}B_9P_2Pt$: C, 46.2; H, 4.8; B, 13.3%).

$3-(Bu^tNC)_2-3,1,2-PdC_2B_9H_{11}$ *and* $3-(NH_3)_2-3,1,2PdC_2B_9H_{11}$. These were obtained by displacement reactions from complexes (**1**) and (**4**) respectively by addition of the free ligand in CH_2Cl_2 and were characterised in solution by their ^{11}B n.m.r. spectra (see Table 1).

X-Ray Crystallography of Complex (**1**).—*Crystal data.* $C_8H_{27}B_9N_2Pd$, *M* = 355.0, monoclinic, space group $P2_1/c$, *a* = 8.474 5(12), *b* = 12.363 6(19), *c* = 16.775 9(26) Å, β = 109.14(1)°, *U* = 1 660.5(4) $Å^3$, *Z* = 4, D_c = 1.42 g cm^{-3}, *F*(000) = 720, $\bar{\lambda}$(Mo-K_α) = 0.710 69 Å, μ(Mo-K_α) = 10.86 cm^{-1}, crystal dimensions 0.25 × 0.10 × 0.07 mm.

Data collection and processing.[25] Syntex $P2_1$ diffractometer, θ—2θ scan mode with variable scan width (1° above K_{α_2} to 1° below K_{α_1}) and scan speed (0.0167 to 0.4883° s^{-1}), graphite monochromated Mo-K_α radiation; 2 772 independent reflections measured (0 < θ < 50°), 2 070 observed [$I > 3\sigma(I)$]. Absorption correction (ABSCOR[28]) gave maximum, minimum transmission factors for correction of $|F_o|$ of 0.987 7(200) and 0.956 3(0,15,2) respectively.

Structure solution and refinement. Patterson and Fourier (heavy-atom) methods.[29] Full-matrix least-squares refinement with non-hydrogen atoms anisotropic[30] gave *R* = 0.045. Fourier difference synthesis revealed all hydrogens, which were then included[31] and the model was further refined (hydrogens isotropic) to R $(=\Sigma[|F_o|-|F_c|]/\Sigma|F_o|)$ = 0.030. A weighting scheme $w = \{1 + [|F_o| - (B/A)]^2\}^{-1}$ with *B* = 65 and *A* = 30 was found suitable and gave a final R' $\{=[\Sigma w(|F_o|-|F_c|)^2/\Sigma w|F_o|^2]^{\frac{1}{2}}\}$ of 0.028.

X-Ray Crystallography of Complex (**2**).—*Crystal data.* $C_8H_{29}B_9P_2Pd$, *M* = 391.0, monoclinic, space group $P2_1/c$, *a* = 6.718 3(10), *b* = 15.502 4(18), *c* = 17.918 4(24) Å, β = 101.90(1)°, *U* = 1 826.1(4) $Å^3$, *Z* = 4, D_c = 1.422 g cm^{-3}, *F*(000) = 792, μ(Mo-K_α) = 11.57 cm^{-1}, crystal dimensions 0.25 × 0.15 × 0.05 mm.

Data collection and processing. As for complex (**1**). Details pertinent to (**2**) are as follows: $2\theta_{max.}$ = 52°, 2 950 recorded independent intensities, 2 214 observed (3σ) reflections; maximum and minimum transmission factors (for the correction of $|F_o|$) 0.974 0(020) and 0.935 6(022).

Structure solution and refinement. Patterson and Fourier (heavy-atom) methods. Full-matrix least-squares refinement with isotropic thermal parameters for all non-hydrogen atoms gave *R* = 0.051. Introduction of anisotropic thermal parameters, and anomalous scattering components[32] for palladium and phosphorus, gave *R* = 0.041. Fourier difference synthesis revealed all hydrogens, which were included with isotropic thermal parameters, and the model was refined further to a final *R* of 0.026. A weighting scheme of the form $w = [1 + 3\sigma^2(F) + 0.02|F_o|]^{-1}$ was found suitable and gave R' = 0.024.

Acknowledgements

We thank the S.E.R.C. for grants in support of this work, Dr. N. W. Alcock for providing *X*-ray facilities, and Dr. D. M. P. Mingos for useful discussions and preprints of his papers.

References

1 H. M. Colquhoun, T. J. Greenhough, and M. G. H. Wallbridge, *J. Chem. Soc., Chem. Commun.*, 1977, 737.
2 M. F. Hawthorne, D. C. Young, T. D. Andrews, D. V. Howe, R. L. Pilling, A. D. Pitts, M. Reintjes, L. F. Warren, and P. A. Wegner, *J. Am. Chem. Soc.*, 1968, **90**, 879.
3 D. M. P. Mingos, M. I. Forsyth, and A. J. Welch, *J. Chem. Soc., Chem. Commun.*, 1977, 605; *J. Chem. Soc., Dalton Trans.*, 1978, 1363.
4 H. M. Colquhoun, T. J. Greenhough, and M. G. H, Wallbridge, *J. Chem. Soc., Chem. Commun.*, 1976, 1019.
5 R. M. Wing, *J. Am. Chem. Soc.*, 1968, **90**, 4828.
6 R. M. Wing, *J. Am. Chem. Soc.*, 1967, **89**, 5599.
7 L. F. Warren and M. F. Hawthorne, *J. Am. Chem. Soc.*, 1968, **90**, 4823.
8 H. M. Colquhoun, T. J. Greenhough, and M. G. H. Wallbridge, *J. Chem. Soc., Dalton Trans.*, 1979, 619.
9 H. M. Colquhoun, T. J. Greenhough, and M. G. H. Wallbridge, *Acta Crystallogr., Sect. B*, 1978, **34**, 2373.
10 D. M. P. Mingos, *J. Chem. Soc., Dalton Trans.*, 1977, 602.
11 F. A. Cotton and G. Wilkinson, 'Advanced Inorganic Chemistry,' 3rd edn., Interscience, New York and London, 1972, p. 720.
12 H. M. Colquhoun, T. J. Greenhough, and M. G. H. Wallbridge, *J. Chem. Soc., Chem. Commun.*, 1978, 322.
13 J. L. Spencer, M. Green, and F. G. A. Stone, *J. Chem. Soc., Chem. Commun.*, 1972, 1178.
14 M. F. Hawthorne and T. D. Andrews, *J. Am. Chem. Soc.*, 1965, **87**, 2496.
15 A. Zalkin, T. E. Hopkins, and D. H. Templeton, *Inorg. Chem.*, 1966, **5**, 1189.
16 H. M. Colquhoun, T. J. Greenhough, and M. G. H. Wallbridge, *Acta Crystallogr., Sect. B*, 1977, **33**, 3604.
17 T. J. Greenhough and M. F. C. Ladd, *Acta Crystallogr., Sect. B*, 1978, **34**, 2744.
18 G. J. Palenik and G. R. Clark, *Inorg. Chem.*, 1970, **9**, 2754.
19 L. Pauling, 'The Nature of the Chemical Bond,' 3rd edn., Cornell University Press, Ithaca, New York, 1960.
20 N. A. Bailey and R. Mason, *J. Chem. Soc. A*, 1968, 2594.
21 M. L. Schneider and H. M. M. Shearer, *J. Chem. Soc., Dalton Trans.*, 1973, 354.
22 R G. Teller, J. J. Wilczynski, and M. F. Hawthorne, *J. Chem. Soc., Chem. Commun.*, 1979, 472.
23 G. A. Barclay, R. S. Nyholm, and R. V. Parish, *J. Chem. Soc.*, 1961, 4433.
24 P. A. Wegner and M. F. Hawthorne, *Chem. Commun.*, 1966, 861.

25 H. M. Colquhoun, T. J. Greenhough, and M. G. H. Wallbridge, *J. Chem. Soc., Dalton Trans.*, 1978, 303.
26 F. G. Mann and H. R. Watson, *J. Chem. Soc.*, 1958, 2772.
27 F. G. Mann and A. F. Wells, *J. Chem. Soc.*, 1938, 702.
28 N. W. Alcock, 'Crystallographic Computing,' eds. F. R. Ahmed, S. R. Hall, and C. P. Huber, Munksgaard, Copenhagen, 1970, pp. 271—278.
29 *X*-RAY, Technical Report TR-192, ed. J. M. Stewart, Computer Science Centre, University of Maryland, 1972.
30 D. T. Cromer and S. B. Mann, *Acta Crystallogr., Sect A*, 1968, **24**, 321.
31 R. F. Stewart, E. R. Davidson, and W. T. Simpson, *J. Chem. Phys.*, 1965, **42**, 3175.
32 D. T. Cromer and O. Liberman, *J. Chem. Phys.*, 1970, **53**, 1891.

Received 8*th June* 1984; *Paper* 4/958